MEASUREMENT SCIENCE REVIEW, **17**, (2017), No. 2, 61-67

DE GRUYTER OPEN

MEASUREMENT SCIENCE REVIEW

Journal homepage: http://www.degruyter.com/view/j/msr

ISSN 1335-8871

Field Programmable Gate Array (FPGA) Respiratory Monitoring System Using a Flow Microsensor and an Accelerometer

Idir Mellal[1], Mourad Laghrouche[1], Hung Tien Bui[2]

[1]*Mouloud Mammeri University, Faculty of electrical engineering and computing science, PO Box 17 RP 15000, Tizi Ouzou, Algeria. Lampa laboratory, larouche_67@yahoo.fr*

[2] *University of Québec At Chicoutimi, G7H-2B1, Chicoutimi, Canada*

This paper describes a non-invasive system for respiratory monitoring using a Micro Electro Mechanical Systems (MEMS) flow sensor and an IMU (Inertial Measurement Unit) accelerometer. The designed system is intended to be wearable and used in a hospital or at home to assist people with respiratory disorders. To ensure the accuracy of our system, we proposed a calibration method based on ANN (Artificial Neural Network) to compensate the temperature drift of the silicon flow sensor. The sigmoid activation functions used in the ANN model were computed with the CORDIC (COordinate Rotation DIgital Computer) algorithm. This algorithm was also used to estimate the tilt angle in body position. The design was implemented on reconfigurable platform FPGA.

Keywords: Accelerometer, CORDIC, FPGA, respiratory monitoring, ANN, SPI, MEMS flow sensor.

1. INTRODUCTION

Respiration is one of the most important vital signs of a person. A continuous and automatic monitoring system can be a needful instrument for medical staff, especially for monitoring patients affected by respiratory diseases. In addition, simultaneous monitoring of respiratory function and activity level may be beneficial in the monitoring of chronic conditions such as chronic obstructive pulmonary disorder [1]-[2]. Hence, the development of monitoring systems has become a topical issue [1]-[7]. In the literature, many studies have explored respiration monitoring. Backer et al. [8] investigated the different physiological and technical methods of implementing respiratory monitoring systems. Other works based on different approaches have been performed particularly in engineering. Binu et al. [9] proposed a monitoring system using a thermal flow sensor, tri-axial accelerometer, and photo electric sensor to measure the air flow, the body posture, and the oxygen saturation, respectively. In 2014, Rong et al. [10] integrated 3 micro sensors with mobile communication devices including hot-film flow sensor, accelerometer, and oximeter. They built a real-time system for monitoring and diagnosing obstructive sleep apnea. The use of the silicon flow sensor and a tri-axial accelerometer placed on the torso can measure the respiration rate and the chest movement [3]-[7]. MEMS components have found increasing use in medical applications. MEMS devices offer uniqueness in their application, fabrication, and functionality. The thermal flow sensor is one of the few devices, allowing the measurement of the gas flow velocity. A miniature hot wire sensor has been recently constructed using MEMS technologies [11]-[13]. The major drawback of this type of sensor is the dependence of its characteristics on ambient temperature.

The temperature compensation methods of the silicon sensor can be divided into three methods: software, hardware, and hybrid. The software method is based on data processing and algorithms such as the ANN technique [14]-[16]. The hybrid method uses both approaches to realize the compensation. The hardware method is much more efficient and easier. It can be achieved using analog or digital signal conditioning circuits. Digital signal conditioning circuits need A/D and D/A conversion blocks that lead to considerable consumption of chip area. Other methods for digital implementation such as ASIC (Application Specific Integrated Circuit), DSP (Digital Signal Processing), and FPGA can be used. DSP-based implementations are not suitable for modeling the parallel behavior of the neurons because of their sequential nature. ASIC implementation is more efficient than FPGA in terms of power and area consumption, but it suffers from a lack of reconfigurability [17].

In this paper, we propose an alternative approach based on employing an artificial neural network for compensating the temperature-drift of the output flow sensor. The neurons in

DOI: 10.1515/msr-2017-0008

the hidden layer of the ANN model use the sigmoid activation function which has been computed with the CORDIC algorithm [19]. This algorithm proposed by Volder [20] is a simple and efficient method to calculate the trigonometric and hyperbolic function through coordinate transformation [21]-[23]. It has been used in both the temperature compensation of the flow sensor and the body position measurement. The tri-axial accelerometer is used to assess the physical activity and measure the chest movement. The accelerometer data will be transmitted with an SPI (Serial Peripheral Interface) interface that is used to compute the tilt angle and show the XYZ positions. To reduce the computational complexity and release the memory, we used a 2D CORDIC-based algorithm for the tilt angle calculations by means of the inverse tangent function. In adopting this approach, an effort has been made to fulfill the procedure in less time while maintaining high accuracy for the implementation [19]. Using the VHDL language, we developed, in this work, an FPGA implementation of a respiratory monitoring system combining a calibrated flow sensor and a tri-axial accelerometer. The tilt angle is computed with the CORDIC (Coordinate Rotation DIgital Computer) algorithm with high accuracy. To ensure the accuracy of our model, we used a CORDIC algorithm for computing a sigmoid and the inverse tangent functions. The whole mixed system is implemented on Altera FPGA DE2 board.

2. MATERIALS & METHODS

Our system contains the flow sensor with its different parts and a digital accelerometer, BMA180, with the CORDIC core to compute the tilt angle and show the XYZ position. Many works have been done to validate and test the sensors. The reliability of the sensor has been tested and various tests have been performed on the final structure [24]. Test and verification of the design were carried out by implementing the proposed technique for temperature compensation and computing the tilt angle on a reconfigurable platform based on an FPGA device. In addition to the 3 outputs of the system: tilt angle, XYZ positions and the air flow, we can add another intelligent block for other health disorders. The proposed system can be used by people suffering from apnea syndrome, asthma, or Chronic Obstructive Pulmonary Disease (COPD).

A. Description of the flow sensor

A miniature hot wire sensor has been constructed using MEMS technologies [11]-[13]. Fig.1. shows the final structure of the hot wire sensor obtained at the end of the process. First, PECVD (Plasma Enhanced Chemical Vapor Deposition) silicon nitride was deposited on p type 4" wafers to a thickness of 0.3 µm. Then, the silicon nitride film was patterned, and wet thermal oxidation of silicon made through the nitride window. Oxidation time was adjusted with technological step simulation for achieving a flat surface. A 0.3 µm depth silica cavity was obtained. Polycrystalline silicon was deposited (LPCVD – thickness 0.5 µm) and doped by boron ion implantation. After the thermal annealing, polycrystalline silicon was patterned into variable section wire. Electrical contacts were finally taken with chromium pads. The releasing of the wire was performed by wet-etching of the silica cavity after dicing the sensors. The reliability of the sensor was discussed by Bensidhoum et al. [24]. The power consumption is less than 10 mW. The size of the hot wire is (50 x 2x 0.5) μm^3. This sensor can be used as temperature or air flow sensor (Hot wire anemometer). The Temperature Coefficient of Resistance (TCR) is roughly around 0.14 %/°C.

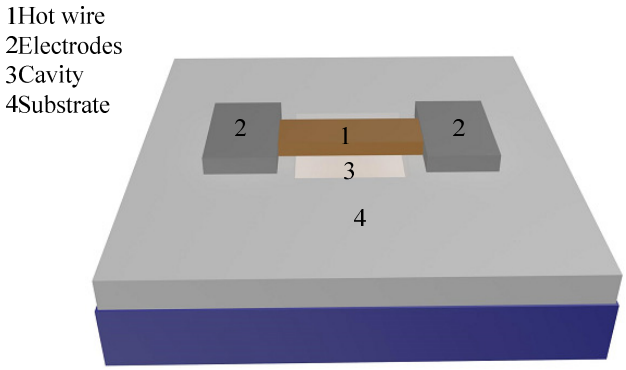

Fig.1. Description of the hot wire sensor.

B. The accelerometer

The accelerometer is a popular device used in many fields, especially in biomedical application. It can be used as a body-motion sensor to detect the physical motion parameters and the respiratory rate that can be used in many applications. In this work, the parameter of interest is the tilt angle. This can be computed using a commercial digital accelerometer sensor, BMA180, presented in Fig.2. The classical method of rectangular (x, y, z) to spherical (ρ, θ, φ) conversion can be used to relate the tilt angle θ [25].

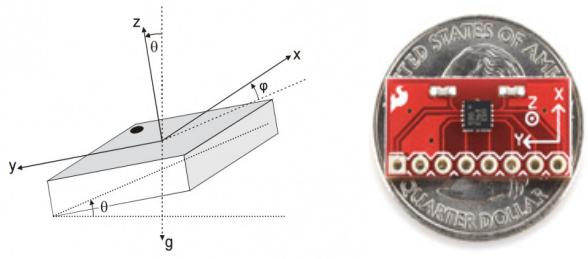

Fig.2. Representation of the BMA180 accelerometer [25].

As all other MEMS sensors, the BMA180 outputs show a high-frequency noise. The planned work consisted in implementing a Kalman filter on the FPGA to filter the accelerometer outputs and remove the high frequencies. But the power consumption, the utilized resources and the size of the device will increase, and this is not convenient for a wearable device. For this reason, we used the programmable integrated filters available on the BMA180.

C. The Altera DE2 development board

For the proof of concept, the FPGA design was implemented on the Altera DE2 board. It is a development board that contains the Cyclone II FPGA chip and contains many other devices and I/Os. Once the design is validated, the following step will be to design a custom FPGA board for the final system. The used peripherals and its connection to the Cyclone II FPGA are shown in Fig.3. [26].

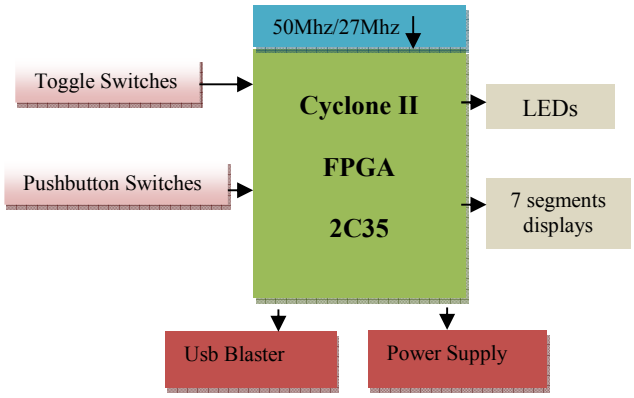

Fig.3. The DE2 development board and the used peripherals: we used the toggle and the pushbutton switches.

3. HARDWARE IMPLEMENTATION

The compensation of the flow sensor is achieved by using the ANN model and it is implemented on the FPGA with the CORDIC algorithm to compute the accelerometer output.

There are different methods of implementing an ANN and CORDIC in hardware: digital, analog, and hybrid, each one has advantages and disadvantages.

The analog method offers a low propagation time, low power consumption and small chip area of silicon. But it suffers from thermal drift, inexact computation results and lack of reprogrammability. The digital implementation offers a good precision of computing, true parallel implementation, and powerful software development tools [15], [21], [23]. It is important to note that ANNs require parallel computation. They are inspired by biological neural systems. Fig.4. presents the different devices used and the signal conditioning blocks of the sensors.

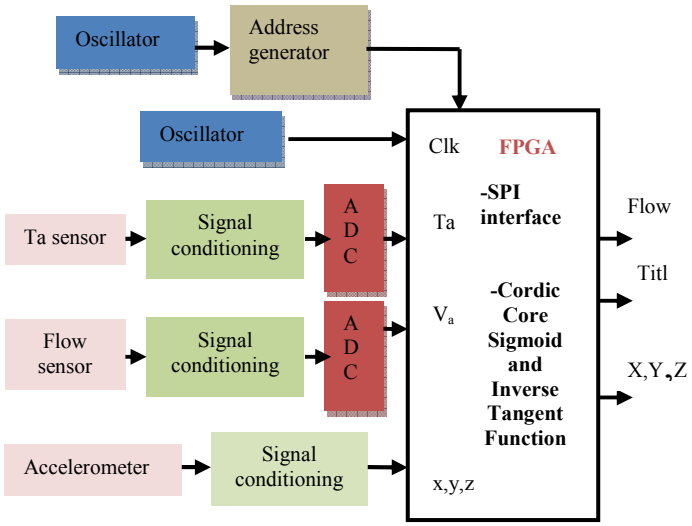

Fig.4. The architecture of the system: Va is the air velocity and Ta is the air temperature.

The oscillators are used to generate the clock and different addresses used for selection. The conditioning circuit contains: amplifier, filter, sample and hold circuits. Both ADC and DAC are used to convert the data in and data out of the FPGA. The architecture of the BMA 180 block is shown in Fig.5.

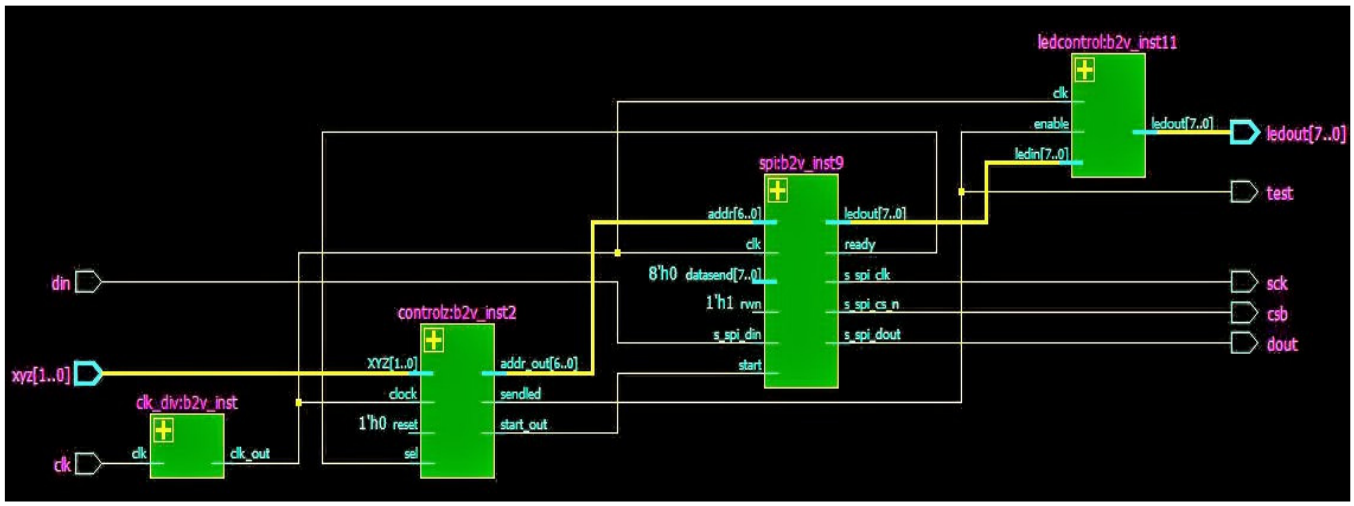

Fig.5. The architecture of the BMA180 block: we implemented the SPI protocol to carry out the data. The control block generates the clock and the addresses signals.

A. Temperature compensation and test

The probe embedded with MEMS hot-film sensors was calibrated in a closed-circuit wind tunnel. A free-stream turbulence level in the test section is very low and temperature can be controlled with a precision of ±0.5°C. Fig.6. illustrates the wind tunnel, the different wind speeds were generated from 0 m/s to 35 m/s with a step of 1 m/s.

The experiments were conducted and repeated in a room with different air temperatures 15°C, 20°C, 25°C, 30°C, 35°C, respectively. Fig.7. shows the calibration of the MEMS flow sensor with different air temperature. The characteristics of the flow sensor face two difficulties, the first difficulty is the compensation for the fluid temperatures and the other is the linearization of highly nonlinear responses. To compensate the temperature effect on the output of the sensor, the circuit should be modeled. This modeling can be achieved using inverse modeling of ANN [14]-[16].

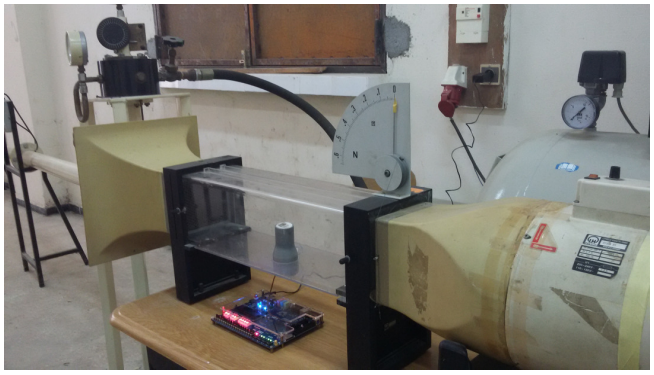

Fig.6. Wind tunnel calibration or the hot wire sensor.

Fig.8. shows the block diagram of ANN based compensation scheme for the hot wire sensor using the inverse model.

For training the neural network, the standard back propagation learning algorithm was used. Multi Layer Perceptron (MLP) is an ANN which employs three layered perceptron based on a feed forward network with signal processing neurons in its hidden and output layers. The input layer had two inputs and a bias. The number of neurons in the hidden layer was fixed at six after performing several tests. The data set used for learning and testing the ANN was composed of 310 and 90 elements, respectively. The selection of the number of neurons in the hidden layer was done on the basis of minimum Mean Square Error (MSE), weight factor and bias values suitable for hardware implementation and its dynamic range. Moreover, the number of neurons was kept as small as possible for simplicity in circuit implementation at the subsequent stage. Fig.9. presents the ANN model with two blocks. The Multiplier-accumulator block and the transfer function block. The activation function was computed with the CORDIC Algorithm. The implementation of the ANN model on the FPGA board is shown in Fig.10.

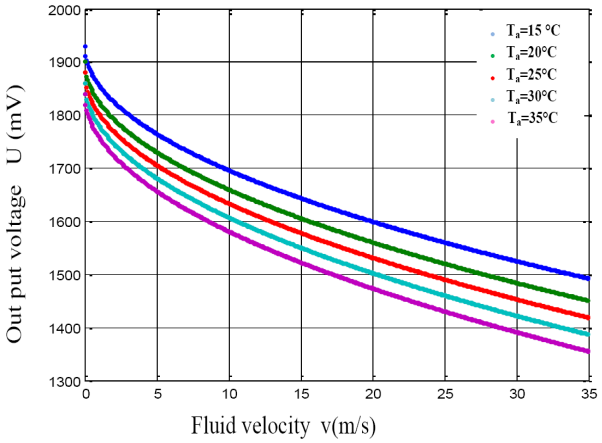

Fig.7. The response of the flow sensor for different temperatures.

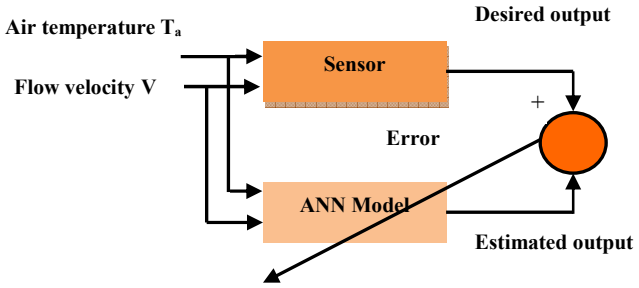

Fig.8. The scheme of the ANN compensation model: the ANN model corrects the output of the sensor by comparing the desired and the estimated output.

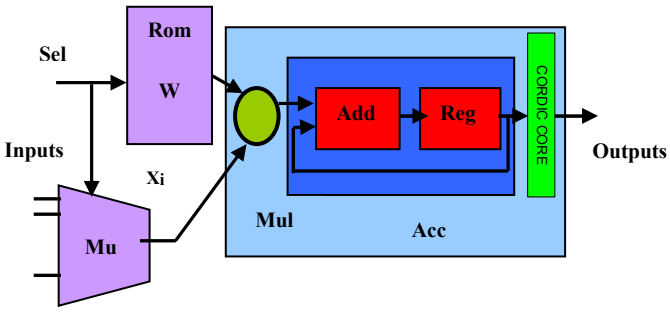

Fig.9. The neural blocks: the transfer function Sigmoid of the neuron was computed using CORDIC. A ROM memory was used to store the neuron weights, then multiply each input with the corresponding weight using the MAC (Multiplier- Accumulator).

Fig.11. shows the response of the micro flow sensor after the compensation and the linearization. After correction the maximum non-linearity of the output signal is less than 0.35 %, its resolution is 0.07 V/m.s^{-1}.

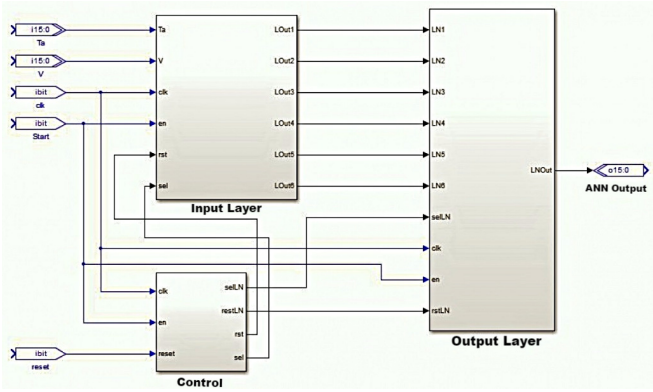

Fig.10. The Architecture of ANN implementation: the input layer is composed of 6 neurons with a sigmoid transfer function. The output layer contains one neuron with a linear transfer function. The control block generates the control and selection signals.

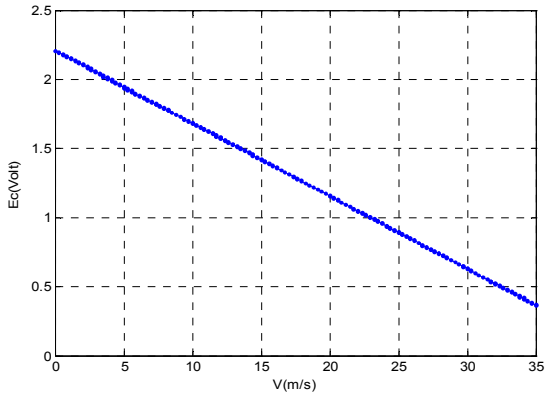

Fig.11. The response of the flow sensor after compensation and linearization

B. Tilt measurement

The BMA 180 was used to compute the tilt angle using the CORDIC algorithm (COrdinate Rotation DIgital Computer) and the inverse tangent function [22], [23]. Two basic CORDIC modes are used to compute different functions: the rotation mode and the vectoring mode [19]. The rotation-mode CORDIC determines the coordinates of any given vector after rotation through a given angle, while in the vectoring-mode it computes the magnitude and phase of the vector. The unified algorithm for linear and hyperbolic CORDICs is an extension of the basic CORDIC algorithm for circular trajectory. It is based on the generalized principle proposed in [19] to include hyperbolic and linear trajectories along with the original circular trajectory of operation. If the micro-rotation angles are restricted to $\tan^{-1}(\theta) = \pm 2^{-i}$, the multiplication is reduced just to a shift operation. That is the main advantage of the hardware CORDIC implementation. In our case; the inverse tangent function, $\theta = \text{atan}(Y/X)$, was directly computed using the vectoring mode of the CORDIC algorithm.

$$Zi = Z_0 + \tan^{-1}(Y_0/X_0) \quad (1)$$

By setting the parameters of the function to have a vectoring mode and $Z_0 = 0$, we managed to compute the $\text{atan}(Y_0/X_0)$ function using equation 1. The properties of the inverse tangent function can be implemented to simplify the architecture.

C. The data representation

Two Complement Fixed Point Format is used for representing the data and computing the outputs. The number of bits chosen for this work is 12 bits. The s2.9 representation is used with one sign bit (Sn), 2 integer bits (I0 to I1) and 9 fractional bits (f0 to f7) as shown in Table 1.

Table 1. Data structure.

Sign	I1	I0	F0	……..	F8
Sign bit	Integer part			Fraction part	

Radix point

Table 2. shows 2 numbers, with different signs.

Table 2. Numbers representation.

Format	Binary	Hexa	Decimal
S2.9	000011101101	0ED	0.4636
S2.9	111100000110	F06	-0.2449

To perform an efficient implementation the fixed point data is used, as shown previously. The accelerometer output is 8 bits, it is important to convert it to 12 bits. For this reason, we use a data converter. A sign extension is performed (the MSB bit). The following examples demonstrate the conversion from 8 to 12 bitswords.

X8= 0xxx xxxx ====> X12= 0000 0xxx xxxx
X8= 1xxx xxxx ====> X12= 1111 1xxx xxxx

Fig.12. shows the machine state of the control block. Each circle corresponds to a state and the transition between two states is represented by a directed arc.

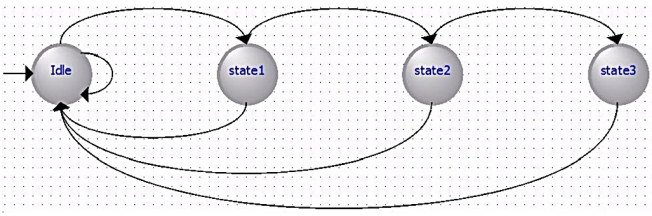

Fig.12. State diagram description of the control block.

The first state represents the idle state of the system. The transition to state1 is activated by the enable signal "en" and the rising edge clock. The sensors collect the data. The transition to the second state is activated by the signal "sel". The first layer of the ANN is selected and the tilt angle is computed using the accelerometer data. The transition to state 3 is performed by the "selLN" signal. The system will return to its idle state regardless of its present state activated

by using the signal "reset". Fig.13. shows the resources consumption on the Altera Cyclone II 2C35 FPGA device. We notice the available resources after the implementation.

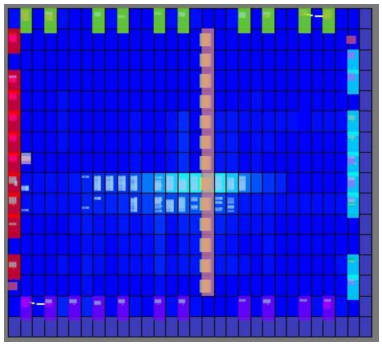

Fig.13. The resources consumption of the FPGA: the total wire utilization is 48 %.

4. RESULTS AND DISCUSSION

A respiratory monitoring system was developed using a flow sensor and a tri-axis accelerometer. The SPI (Serial Peripheral Interface) was used to obtain the data from the accelerometer for the wearable system. The SPI protocol was also implemented. The estimated error was less than 1°; $\Delta\theta = 0.89°$. It was calculated after several steps of execution of the CORDIC core. Table 3. shows the resource consumption in the FPGA.

Table 3. The resource consumption.

Registers	Pins	Logic elements	Memory
363	73/315	250 / 4,608	0

To verify the monitoring and diagnosing respiratory diseases, a series of monitoring and diagnostic tests was conducted during a pulmonary breathing cycle for a man (35-year-old). Fig.14. shows the response of the flow sensor using a nasal cannula. Due to the small dimensions of the flow sensor, we managed to introduce it in the nasal cannula to measure the flow of inspiration and expiration.

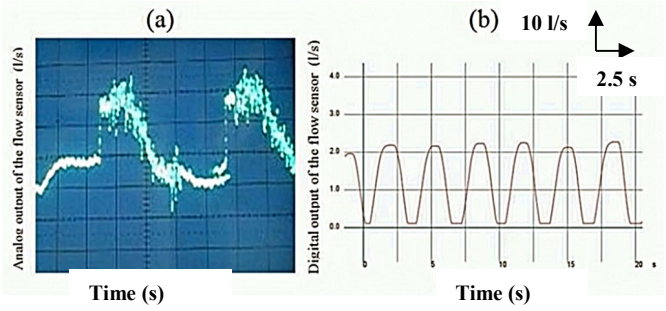

Fig.14. Flow sensor response using nasal cannula: a) the analog output for two breath cycles b) the digital output for 6 breath cycles.

Fig.15. shows the outputs of the accelerometer which is placed on the chest of the subject so that the X-axis is perpendicular to the body. The data were recorded in the laboratory during 15 min for three different positions: sitting, standing and lying supine. In future works, we aim to develop a dedicated SOC (System On Chip) to respiratory monitoring with high performances: low consumption, small size, and low cost.

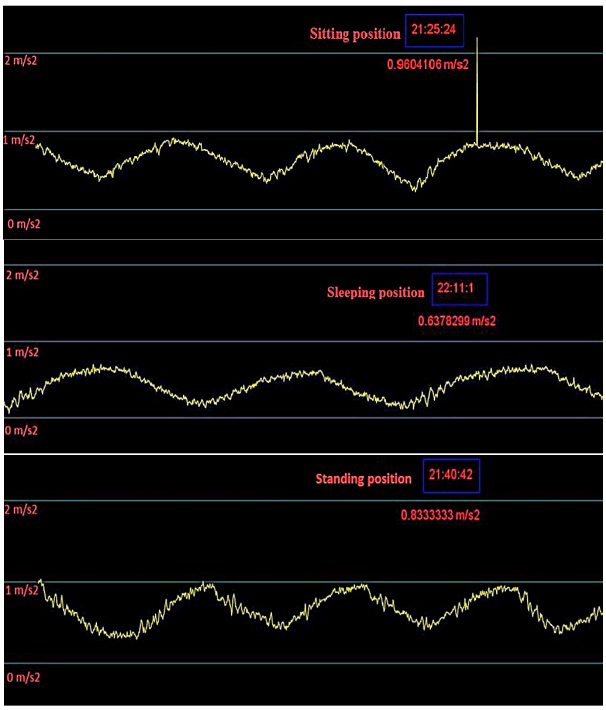

Fig.15. Accelerations along the X-axis for different positions: sitting, standing and lying supine.

Fig.14. and Fig.15. show the outputs of our system. We can see the similarity between the analog output and the digital output. Moreover, the accelerometer output can be extended for many body postures.

5. CONCLUSION

We have proposed a mixed system to monitor the respiratory activity. The monitoring system is based on mixing a flow sensor and a 3Axis accelerometer as a motion sensor. The CORDIC algorithm was used to compute the tilt angle and approximate the sigmoid function. The inverse tangent function is used to compute the tilt angle to estimate the body positions. An FPGA implementation is made on the DE2 board using the VHDL language. We have found that the respiratory intensity and the pulmonary rhythm are closely linked. The hardware implementation shows that the physical resource consumption was acceptable and the observed error was less than 1°. Therefore, this system can be extended to include other sensors and modules to serve in daily homecare endowed with the SPI interface. In future works, we aim to develop a dedicated SOC for respiratory monitoring with high performances: low consumption, small size, and low cost.

REFERENCES

[1] Vandenbussche, N.L., Overeem, S., Johannes, P., van. Dijk, J.P., Simons, P.J., Pevernagie, D.A. (2015). Assessment of respiratory effort during sleep: Esophageal pressure versus noninvasive monitoring techniques. *Sleep Medicine Reviews*, 24, 28-36.

[2] Chattopadhyay, M., Chowdhury, D. (2016). A new scheme for reducing breathing trouble through MEMS based capacitive pressure sensor. *Microsystem Technologies*, 22 (11), 2731-2736.

[3] Zadeh, E.G., Gholamzadeh, B., Charca, G.A. (2016). Toward spirometry on chip: Design, implementation and experimental results. *Microsystem Technologies*, doi: 10.1007/s00542-016-3200-0.

[4] Shany, T., Redmond, S.J., Narayanan, M.R., Lovell, N.H. (2012). Sensors-based wearable systems for monitoring of human movement and falls. *IEEE Sensors Journal*, 12 (3), 658-670.

[5] Luo, J., Wang, Z., Shen, Ch., Wen, Z., Liu, S., Cai, S., Li, J. (2015). Rotating shaft tilt angle measurement using an inclinometer. *Measurement Science Review*, 15 (5), 236-243.

[6] Nam, Y., Park, J.W. (2013). Child activity recognition based on cooperative fusion model of a triaxial accelerometer and a barometric pressure sensor. *IEEE Journal of Biomedical and Health Informatics*, 17 (2), 420-426.

[7] Cao, Z., Zhu, R., Que, R.Y. (2011). A wireless portable system with microsensors for monitoring respiratory diseases. *IEEE Transaction on Biomedical Engineering*, 59 (11), 3110-3116.

[8] Becker, D.E., Casabianca, A.B. (2009). Respiratory monitoring: Physiological and technical considerations. *Anesthesia Progress*, 56 (1), 14-22.

[9] Binu, E., Varsha, N.S. (2014). Real time monitoring of respiratory parameters using a wireless portable system. *International Journal of Engineering Development and Research*, 3 (1), 283-287.

[10] Zhu, R., Cao, Z., Que, R. (2014). Integration of micro sensors with mobile devices for monitoring vital signs of sleep apnea patients. In *9th IEEE International Conference on Nano/Micro Engineered and Molecular Systems (NEMS)*, April 13-16, 2014. IEEE, 462-466.

[11] Laghrouche, M., Montes, L., Boussey, J., Ameur, S. (2011). Low-cost embedded spirometer based on micro machined polycrystalline thin film. *Flow Measurement and Instrumentation*, 22 (2), 126-130.

[12] Laghrouche, M., Montes, L., Boussey, J., Meunier, D., Ameur, S., Adane, A. (2011). In situ calibration of wall shear stress sensor for micro fluidic application. In *Proceedings of Eurosensors XXV*, September 4-7, 2011, Athens, Greece.

[13] Makhlouf, S., Laghrouche, M., Adane, A.E.H. (2016). Hot wire sensor-based data acquisition system for controlling the laminar boundary layer near plant leaves within a greenhouse. *IEEE Sensors Journal*, 16 (8), 2650-2657.

[14] Jun, S., Kochan, O. (2014). Investigations of thermocouple drift irregularity impact on error of their inhomogeneity correction. *Measurement Science Review*, 14 (1), 29-34.

[15] Mellal, I., Laghrouche, M., Idjeri, B., Beguenane, R., Ameur, S. (2012). Implementation of ANN in FPGA for improved temperature drift of the MEMS flow sensor. *Sensors & Transducers Journal*, 145 (10), 1-9.

[16] Laghrouche, M., Idjeri, B., Hammouche, K., Tahanout, M., Boussey, J., Ameur, S. (2012). Temperature compensation of micromachined silicon hot wire sensor using ANN technique. *Microsystem Technologies*, 18 (3), 237-246.

[17] Wanhammar, L. (1999). *DSP Integrated Circuits*. Academic Press.

[18] Valls, J., Kuhlmann, M., Parhi, K.K. (2002). Evaluation of CORDIC algorithms for FPGA design. *Journal of VLSI Signal Processing Systems for Signal, Image and Video Technology*, 32 (3), 207-222.

[19] Tiwari, V., Khare, N. (2015). Hardware implementation of neural network with Sigmoidal activation function using CORDIC. *Microprocessors and Microsystems*, 39 (6), 373-381.

[20] Volder, J.E. (1959). The CORDIC trigonometric computing technique. *IRE Transactions on Electronic Computers*, EC-8 (3), 330-334.

[21] Walther, J.S. (1971). A unified algorithm for elementary functions. In *Proceedings of Spring Joint Computer Conference*, May 18-20, 1971, 379-385.

[22] Kumar, N., Sappal, A.S. (2011). Cordinate rotation digital computer algorithm: Design and architectures. *International Journal of Advanced Computer Science and Applications*, 2 (4), 68-71.

[23] Liao, W.-T., Lin, W.-Y., Cheng, W.-C., Lei, K.F., Lee, M.-Y. (2013). Precision enhancement and performance evaluation of a CORDIC-based tilting angle identification algorithm for three-axis accelerometers. In *International Symposium on Biometrics and Security Technologies (ISBAST)*, July 2-5, 2013. IEEE, 187-192.

[24] Bensidhoum, M.T., Laghrouche, M., Sidi Said, A., Montes, L., Boussey, J. (2014). Fabrication flaws and reliability in MEMS thin film polycrystalline flow sensor. *Microsystem Technologies*, 20 (1), 1-7.

[25] SparkFun Electronics. *Triple Axis Accelerometer Breakout - BMA180*. https://www.sparkfun.com/products/retired/9723.

[26] Altera Corporation. (2006). *DE2 User Manual*. ftp://ftp.altera.com/up/pub/Webdocs/DE2_UserManual.pdf

Received December 22, 2016.
Accepted March 9, 2017.